Supplemental Material

Legends to Online Figures

Figure I. Hypoxic and normoxic CSCs. **A**: FACS-sorted c-kit-positive CSCs were stained by DAPI and Pimo (upper two panels); NBT labeling (lower two panels). Nitroreductase activity in both CSC subsets is shown as mean ± SD. **B** and **C**: Bivariate distribution of forward scatter (FSC) and Mito Tracker (**B**) and TMRE (**C**) probes in CSCs. $Pimo^{pos}$-CSCs (white) and $Pimo^{neg}$-CSCs are shown by confocal microscopy. Nuclei are stained by DAPI (blue). *P<0.05 vs. TMRE Low.

Figure II. Pimo identifies hypoxic cells. **A**: Human CSCs (hCSCs) cultured at different O_2 concentration. Pimo labeling (white) was found in hCSCs exposed to 1% O_2. Data are shown as mean±SD. *,**,†P<0.05 vs. 21%, 10%, and 5% O_2, respectively. **B**: The thymus was employed as positive control for Pimo labeling. The closely packed cells in the thymus are all $Pimo^{pos}$ (white). Nuclei: DAPI, blue. **C**: The number of CSCs per mm^3 of myocardium increases with age in the atria, Base-MR and apex. M, months. *,**,†,§P<0.05 vs. 3M, 24M, Atria, Base-MR, respectively.

Figure III. CD45 in CSCs. In all assays, enzymatically digested cardiac cells were gated on c-kit, and the co-localization with CD45 was determined to exclude cells of bone marrow origin and mast-cells. Bivariate distribution of c-kit and CD45 in CSCs. Less than 2% of c-kit-positive cells are labeled by CD45 and are consistently $Pimo^{neg}$.

Figure IV. TPZ and the hypoxic thymus. **A**: Hematoxylin-eosin staining of the thymus in 3 month-old mice injected with PBS (left panel) or with daily administration of TPZ (right panel). Following TPZ, an extensive loss of cells is apparent. **B**: Thymus weight in young and old mice injected with PBS (blue dots) or TPZ for 4 days (red dots). Data are shown as mean±SD. *P<0.05 vs. PBS.

Figure V. TPZ and cardiac function. Cardiac function measured by invasive hemodynamics in young (Y) and old (O) mice injected with PBS or TPZ. LVSP, left ventricular systolic pressure; LVEDP, LV end-diastolic pressure. Data are shown as mean±SD. *P<0.05 vs. Y.

Figure VI. FACS sorting of $Pimo^{pos}$- and $Pimo^{neg}$-CSCs. Scatter plots illustrate gating for c-kit in CSCs; the distribution of Pimo labeling in CSCs is shown below.

Figure VII. Autofluorescence of formalin-fixed Myocardium. Individual measurements are listed.

Figure VIII. Hyperoxia. **A**: Mice at 26 months of age: distribution of $Pimo^{pos}$- and $Pimo^{neg}$-CSCs at baseline (untreated control, CTRL) and 1, and 7 days after hyperoxia. The horizontal line indicates the population of $Pimo^{pos}$-CSCs. **B**: Quantitative results are shown as mean±SD. *P<0.05 vs. CTRL.

Figure IX. Mobilization of bone marrow cells following intramyocardial delivery of SCF. Mononuclear cells were harvested from the peripheral blood of mice 6 hours after injection of 2.5 μg of SCF. Bivariate distribution of c-kit and bone marrow lineage markers (Lin) including CD3, Gr-1, CD11b, CD45R, and Ter-119. The intramyocardial administration of SCF did not affect the fraction of circulating c-kit-positive-Lin^{neg} and c-

kit-positive-Lin^{pos} blood cells. Data are shown as mean±SD. CTRL, untreated control animals; PBS, control treated with PBS; SCF, stem cell factor-treated animals.

Figure X. Ventricular hemodynamics. Data are shown as mean±SD. See text.

Figure XI. SCF and cardiac weights. Data are shown as mean±SD. *P<0.05 vs. PBS.

Figure XII. Mononucleated and binucleated myocytes. **A** and **B**: Optical sections of myocytes obtained from tissue sections 40 μm in thickness; they illustrate a mononucleated (**A**) and a binucleated (**B**) myocyte. Connexin 43 (Cx43, green) delineates the cell boundary. The number in each image corresponds to the focal plane in μm. Nuclei, arrowheads.

Methods

Detection of Pimonidazole (Pimo) Positive and Negative CSCs

All protocols were approved by the Institutional Animal Care and Use Committee of the Brigham and Women's Hospital. Animals received humane care in compliance with the "Guide for the Care and Use of Laboratory Animals" as described by the Institute of Laboratory Animal Research Resources, Commission on Life Sciences, National Research Council.

Male C57BL/6 mice at 3, 24, and 30 months of age were injected i.p. with 120 mg/kg b.w. of pimonidazole (Pimo) hydrochloride (Hypoxyprobe-1 kit, hip).[1,2] Control animals received PBS. Two hours following Pimo or PBS administration, mice were anesthetized by inhalation with isoflurane, 1.5% mixed with 100% O_2, and sacrificed. The abdominal aorta was cannulated with a polyethylene catheter, PE-50, filled with a phosphate buffer, 0.2 M, pH 7.4, and heparin, 100 U/ml. In rapid succession, the heart was arrested in diastole by the injection of 0.15 ml of $CdCl_2$, 100 mM, through the aortic catheter, the thorax was opened, perfusion with phosphate buffer was started, and the vena cava was cut to allow drainage of blood and perfusate. After perfusion with phosphate buffer for 2 minutes, the coronary vasculature was perfused for 15 minutes with formalin. Heart and thymus were then excised, and weights were recorded.[3-6]

Formalin-fixed paraffin-embedded myocardial sections were labeled with c-kit (R&D) and α-sarcomeric actin (Sigma) antibodies to identify CSCs and cardiomyocytes, respectively. Nuclei were stained by DAPI. The localization of Pimo in CSCs was determined with the anti-PIM, Hypoxyprobe-1 kit (hpi) and cycling CSCs were recognized by labeling with Ki67 antibody (Vector). The thymus was employed as a positive control for Pimo immunostaining (Online Table I).

The number of Pimo^{pos} and Pimo^{neg} c-kit-positive CSCs per unit volume of myocardium in the atria, base mid-region (Base-MR), and apex of the left ventricle (LV) was determined according to the Schwartz-Saltykov protocol. This analysis involves the acquisition of the distribution of the diameters of CSC profiles in tissue sections, from which the value per unit volume is subsequently computed[4,5,7,8]

Nitroreductase Activity, and Mitochondrial Content and Inner Transmembrane Potential

The heart of Pimo-injected mice at 3 months of age was enzymatically dissociated, and c-kit-positive CSCs were analyzed by flow-cytometry. FACS-sorted CSCs were incubated at 37°C for 5 minutes with NBT, 1.2 mM, MgCl, 0.05M, NADPH, 2.4 mM, and menadione, 20μM (vitamin K).[9] Cells were then fixed in 2% paraformaldehyde (PFA), permeabilized with 0.5% Triton, and exposed to Pimo antibody. The localization of NBT staining, which is a marker of nitroreductase enzymatic activity, was assessed in $Pimo^{pos}$-CSCs and $Pimo^{neg}$-CSCs.

The fluorescent probes MitoTracker Green FM (Molecular Probes) and tetramethylrhodamine ethyl ester (TMRE; Molecular Probes) were employed to evaluate, respectively, mitochondrial content and membrane potential in CSCs.[10,11] Cells were incubated at 37°C for 30 minutes with 200 nM of MitoTracker Green or 50 nM of TMRE and then analyzed by flow-cytometry. CSCs with high and low positivity for each of the probes were sorted separately, fixed, permeabilized, and exposed to Pimo antibody. The distribution of Pimo in CSCs was assessed by immunolabeling and confocal microscopy.

Human CSCs and Hypoxia

Discarded myocardial specimens were harvested from patients who underwent coronary bypass surgery.[12] The tissue was enzymatically dissociated to obtain single cell suspensions. Small cardiac cells were selected for c-kit with immunomagnetic beads (Miltenyi) or FACS. C-kit-positive human CSCs were cultured in F12K medium supplemented with 10% fetal bovine serum in the presence of 1%, 5%, 10%, or 21% O_2, fixed, permeabilized, and incubated with Pimo antibody. This analysis performed by confocal microscopy allowed us to define the relationship between O_2 levels and Pimo labeling of CSCs.

Identification of Hypoxic Niches

The localization of Pimo and the expression of HIF-1α and CAIX was assessed in cardiomyocytes and fibroblasts surrounding $Pimo^{pos}$- and $Pimo^{neg}$-CSCs (Online Table I). This analysis was performed in tissue sections by immunolabeling and confocal microscopy.

Functional Properties of $Pimo^{pos}$- and $Pimo^{neg}$-CSCs

This assay was done in freshly isolated CSCs obtained from mice at 3 and 30 months of age injected with Pimo. For enzymatic dissociation, hearts were placed on a stainless steel cannula for retrograde perfusion through the aorta as repeatedly done in our laboratory.[4-6,8,13] At completion of digestion, myocytes were enriched by centrifugation and small cardiac cells were collected in the supernatant. Small cells were fixed in 2% PFA for 10 minutes at room temperature, permeabilized with 0.5% Triton, and incubated with antibodies recognizing c-kit (FITC-conjugated, BD Pharmingen), Pimo (Hypoxyprobe-1 kit, hip), Ki67 (DAKO), GATA4 (Santa Cruz), Nkx2.5 (Santa Cruz), and $p16^{INK4a}$ (Santa Cruz) (Online Table I). Flow cytometry was performed with FACSAria (Becton Dickinson), or FACSCanto II (Becton Dickinson) instruments. Cellular debris and aggregates were gated out based on forward and side scatter. Gating on the signal of the nuclear stain DAPI was used to exclude additional artifacts and gating on the signal for c-kit was employed to restrict the analysis to CSCs. Isotype-matched negative controls were utilized to define the threshold for each specific signal and establish the appropriate gate. Data were analyzed with the instrument software.

Capillary Density

To measure the density of capillaries and their distribution with respect to Pimo^{pos}-CSCs and Pimo^{neg}-CSCs, 60 μm thick sections were acquired from hearts of mice at 3 and 26-30 months of age. Endothelial cells were identified by staining with isolectin B4 from Griffonia simplicifolia (Sigma) and CSCs by c-kit together with Pimo labeling. This analysis was performed by two-photon microscopy. A series of optical sections 1 μm apart were obtained throughout the thickness of the specimen and the collected images were converted into three dimensional structures by Imaris software to establish the distance between Pimo^{pos}-CSCs and Pimo^{neg}-CSCs and the closest isolectin-positive cell.[14,15] Additionally, capillary density per mm^2 of myocardium was determined by counting the number of isolectin-positive cells within the optical field.

Depletion of Hypoxic Pimo^{pos}-CSCs

Mice at 3 and 30 months of age were injected daily with tirapazamine (TPZ) (30 mg/kg b.w.; International Laboratory) dissolved in PBS.[16,17] One group of animals at each age interval received a single injection of TPZ and was sacrificed one day later (day 1). Two additional groups of mice were treated for 4 days and sacrificed 1 (day 5) and 8 days (day 12) following the last administration of TPZ. Control mice received PBS. All animals were injected with Pimo 2 hours prior to sacrifice. Hearts were excised and fixed for immunolabeling and confocal microscopy or enzymatically digested for FACS analysis. The number of CSCs per unit volume of myocardium was measured in tissue section with the protocol indicated above.[4,5,7,8,14] The percentage of Pimo^{pos} and Pimo^{neg} CSCs, and the fraction of cycling and early committed CSCs were assessed by immunolabeling and flow-cytometry. Ventricular hemodynamics was measured in mice sacrificed at day 12 (see below).

Telomere Length

This parameter was evaluated by Q-FISH and confocal microscopy in CSCs and cardiomyocytes isolated from hearts at 3 and 30 months of age. Small cells were fixed in 2% PFA, permeabilized with 0.5% Triton, and incubated with antibodies recognizing c-kit and Pimo. Pimo^{pos} and Pimo^{neg} CSCs were then sorted by FACS and exposed to a Cy3-peptide nucleic acid (PNA) probe complementary to the telomere DNA sequence. The same protocol was implemented to evaluate telomere length in cardiomyocytes. The fluorescent signals measured in lymphoma cells with short (L5178Y-S, 7 kbp) and long (L5178Y-R, 48 kbp) telomeres were utilized to compute absolute telomere length.[12,18,19]

Long-Term Label Retaining Assay

Mice at 3 months of age were injected i.p. with BrdU (Sigma), 50 mg/kg body weight, at 12 hours intervals for 7 days. One group of animals was sacrificed one hour after the last administration of the halogenated nucleotide (pulse). Two additional groups of mice were similarly treated and sacrificed after a chase period of 2 and 5 months[5,6,20] The fluorescence intensity of BrdU in Pimo^{pos}- and Pimo^{neg}-CSCs was measured by confocal microscopy. BrdU positivity reflected levels of fluorescent signals ≥1,000 units (pixel x average intensity). The autofluorescence of the section together with the signal generated by the irrelevant antibody, employed as a negative control for BrdU staining,

was at most 900 units. BrdU intensity varying from 1,000-3,999 units and from 4,000-10,000 units was assigned to dimly-labeled and brightly-labeled CSCs, respectively.

Hyperoxia

Mice at 26 months of age were kept in hyperoxic chambers, 70% O_2, for 1 and 7 days.[21-23] At sacrifice, the heart was fixed by retrograde perfusion of the aorta and the proportion of $Pimo^{pos}$- and $Pimo^{neg}$-CSCs was measured by immunolabeling and flow-cytometry as discussed above.

Stem Cell Factor (SCF) Administration

Prior to the injection of SCF in the mouse heart, we determined whether intramyocardial delivery of this cytokine promoted mobilization of bone marrow cells.[24] The heart of 3 months old mice was injected at 3-4 different sites with a cumulative dose of 2.5 µg of SCF (Sigma). Control animals received PBS. Six hours later, animals were sacrificed and the peripheral blood was collected. The number of white blood cells was counted with Turk blood diluting fluid (Ricca Chemical Co.) The whole blood was incubated with RBC lysis buffer to remove erythrocytes. The remaining cells were exposed to antibodies recognizing c-kit and hematopoietic lineage markers and analyzed by flow-cytometry. The cocktail of antibodies against bone marrow surface markers included CD3, Gr-1, CD11b, CD45R, and Ter-119 (Bio Legend).

The heart of mice at 26-30 months of age was injected with 1 µg SCF or PBS distributed in 3-4 different sites of the myocardium. Animals were sacrificed 6, 24 and 48 hours later. In these experiments, mice were ventilated and SCF was administrated in an open-chest preparation. Two additional groups of mice received SCF or PBS by echo-guided injection and were studied 21 days later. The hearts of mice sacrificed 6 and 24 hours following SCF or PBS injection was enzymatically dissociated and the proportion of $Pimo^{pos}$- and $Pimo^{neg}$-CSCs was determined by flow-cytometry.

The groups of mice sacrificed at 2 and 21 days received daily injections of BrdU, 10 mg/kg b.w., and the percentage of CSCs and cardiomyocytes positive for the thymidine analog was measured by immunolabeling and confocal microscopy.[5,6,13,15,20] Mice exposed to BrdU for 21 days were characterized by echocardiography and invasive hemodynamics prior to sacrifice and fixation of the heart with formalin (see above).

Cardiac Function

Echocardiography was performed in conscious mice at 26 months of age 21 days after treatment with SCF or PBS using a Visualsonics Vevo 2100 System equipped with a MS550D high frequency (22-55 MHz) linear transducer.[9,12] Video-sequences were recorded from the parasternal short and long axis views. M-mode tracings were obtained in the short axis view at the level of the papillary muscle. End-systolic and end-diastolic ventricular dimensions, wall thickness, and ejection fraction were determined.

Ventricular hemodynamics was measured in two groups of animals: **a)** mice at 30 months of age injected with 4 doses of TPZ and sacrificed 8 days later (day 12); and **b)** mice at 26 months of age treated with SCF and sacrificed 21 days later. In both cases, animals injected with PBS were used as controls. Under isoflurane inhalation (1.5% mixed with 100% O_2) anesthesia, the right carotid artery was cannulated with a microtip pressure transducer (PVR-1045, Millar Instruments) connected to a recorder (MPVS-400; Millar Instruments) and a computer system. The catheter was advanced into the LV

chamber for the evaluation of LV pressures and + and − dP/d*t* in the closed-chest preparation.[4,9,12] Data were acquired with a Chart 5 (ADInstruments) and analyzed with LabChart 7 software (ADInstruments). After the collection of hemodynamic parameters, the diastolic arrested heart was fixed by perfusion with formalin and cardiac weights were obtained (see above). The echocardiographic measurements of LV chamber diameter and wall thickness in diastole and systole were combined with the hemodynamic values of LV pressure to compute systolic and diastolic wall stress: $\sigma = p \times r/2h$, where p is the LV pressure, r is the chamber radius, and h is the wall thickness.[9,12]

Myocyte Volume and Number

Myocardial sections, 40 μm in thickness were stained by α-SA, laminin and connexin 43 to define the myocardial interstitium and the myocyte boundary. These preparations were analyzed by confocal microscopy.[14] Optical sections 1 μm apart were collected and the images were converted into three dimensional structures by Imaris software. By this approach, the proportion of mononucleated, binucleated, and multinucleated cardiomyocytes was determined in each LV. Additionally, the cell area of each mononucleated and binucleated myocyte was utilized together with cell thickness to compute myocyte volume. The number of mononucleated and binucleated myocytes in the LV was derived from the quotient of the LV myocyte mass and the fraction and volume of each myocyte population.

Telomere Length

Telomere length in BrdU-positive and BrdU-negative myocyte nuclei was evaluated in tissue sections by Q-FISH and confocal microscopy, using a peptide nucleic acid probe labeled by Cy3.[25] The fluorescent signals measured in lymphoma cells (L5178Y) with short (7 kbp) and long (48 kbp) telomeres were utilized to compute absolute telomere length. Individual telomere signals in each nucleus were added and divided by the DAPI signal to correct for differences in the nuclear fraction included in the section.

Data Analysis

The number of animals used in each determination and the magnitude of sampling utilized in each quantitative analysis are listed in Online Table II. Data are presented as mean±SD. Significance between two groups was determined by unpaired two-tailed Student's t-test. For multiple comparisons, the ANOVA test was employed. $P<0.05$ was considered significant.

References

1. Khan M, Meduru S, Mostafa M, Khan S, Hideg K, Kuppusamy P. (2010). Trimetazidine, administered at the onset of reperfusion, ameliorates myocardial dysfunction and injury by activation of p38 mitogen-activated protein kinase and Akt signaling. *J. Pharmacol. Exp. Ther*. 2010; 333: 421-429.
2. Nombela-Arrieta C, Pivarnik G, Winkel B, Canty KJ, Harley B, Mahoney JE, Park SY, Lu J, Protopopov A, Silberstein LE. Quantitative imaging of haematopoietic stem and progenitor cell localization and hypoxic status in the bone marrow microenvironment. *Nat. Cell Biol*. 2013;15: 533-543.

3. Rota M, Boni A, Urbanek K, Padin-Iruegas ME, Kajstura TJ, Fiore G, Kubo H, Sonnenblick EH, Musso E, Houser SR, Leri A, Sussman MA, Anversa P. Nuclear targeting of Akt enhances ventricular function and myocyte contractility. *Circ Res*. 2005; 97: 1332-41.
4. Rota M, LeCapitaine N, Hosoda T, Boni A, De Angelis A, Padin-Iruegas ME, Esposito G, Vitale S, Urbanek K, Casarsa C, Giorgio M, Lüscher TF, Pelicci PG, Anversa P, Leri A, Kajstura J. Diabetes promotes cardiac stem cell aging and heart failure, which are prevented by deletion of the p66shc gene. *Circ Res*. 2006 ; 99: 42-52.
5. Urbanek K, Cesselli D, Rota M, Nascimbene A, De Angelis A, Hosoda T, Bearzi C, Boni A, Bolli R, Kajstura J, Anversa P, Leri A. Stem cell niches in the adult mouse heart. *Proc Natl Acad Sci U S A*. 2006; 103: 9226-31.
6. Boni A, Urbanek K, Nascimbene A, Hosoda T, Zheng H, Delucchi F, Amano K, Gonzalez A, Vitale S, Ojaimi C, Rizzi R, Bolli R, Yutzey KE, Rota M, Kajstura J, Anversa P, Leri A. Notch1 regulates the fate of cardiac progenitor cells. *Proc Natl Acad Sci U S A*. 2008; 105: 15529-34.
7. Urbanek K, Quaini F, Tasca G, Torella D, Castaldo C, Nadal-Ginard B, Leri A, Kajstura J, Quaini E, Anversa P. Intense myocyte formation from cardiac stem cells in human cardiac hypertrophy. *Proc Natl Acad Sci U S A*. 2003; 100: 10440-5.
8. Urbanek K, Rota M, Cascapera S, Bearzi C, Nascimbene A, De Angelis A, Hosoda T, Chimenti S, Baker M, Limana F, Nurzynska D, Torella D, Rotatori F, Rastaldo R, Musso E, Quaini F, Leri A, Kajstura J, Anversa P. Cardiac stem cells possess growth factor-receptor systems that after activation regenerate the infarcted myocardium, improving ventricular function and long-term survival. *Circ Res*. 2005; 97: 663-73.
9. Urbanek K, Cabral-da-Silva MC, Ide-Iwata N, Maestroni S, Delucchi F, Zheng H, Ferreira-Martins J, Ogórek B, D'Amario D, Bauer M, Zerbini G, Rota M, Hosoda T, Liao R, Anversa P, Kajstura J, Leri A. Inhibition of notch1-dependent cardiomyogenesis leads to a dilated myopathy in the neonatal heart. *Circ Res*. 2010; 107: 429-41.
10. Simsek T, Kocabas F, Zheng J, Deberardinis RJ, Mahmoud AI, Olson EN, Schneider JW, Zhang CC, Sadek HA. The distinct metabolic profile of hematopoietic stem cells reflects their location in a hypoxic niche. *Cell Stem Cell*. 2010; 7: 380-390.
11. Yu WM, Liu X, Shen J, Jovanovic O, Pohl EE, Gerson SL, Finkel T, Broxmeyer HE, Qu CK. Metabolic regulation by the mitochondrial phosphatase PTPMT1 is required for hematopoietic stem cell differentiation. *Cell Stem Cell*. 2013; 12: 62-74.
12. Bearzi C, Rota M, Hosoda T, Tillmanns J, Nascimbene A, De Angelis A, Yasuzawa-Amano S, Trofimova I, Siggins RW, Lecapitaine N, Cascapera S, Beltrami AP, D'Alessandro DA, Zias E, Quaini F, Urbanek K, Michler RE, Bolli R, Kajstura J, Leri A, Anversa P. Human cardiac stem cells. *Proc Natl Acad Sci U S A*. 2007; 104: 14068-73.
13. Gonzalez A, Rota M, Nurzynska D, Misao Y, Tillmanns J, Ojaimi C, Padin-Iruegas ME, Müller P, Esposito G, Bearzi C, Vitale S, Dawn B, Sanganalmath SK, Baker M, Hintze TH, Bolli R, Urbanek K, Hosoda T, Anversa P, Kajstura J, Leri A. Activation of cardiac progenitor cells reverses the failing heart senescentphenotype and prolongs lifespan. *Circ Res*. 2008; 102:597-606.
14. Anversa, P and Olivetti, G. Cellular basis of physiological and pathological myocardial growth. In *Handbook of Physiology* (ed. Page E., Fozzard H. A.,

Solaro R.J.). Section 2, The Cardiovascular System, vol. I, The Heart. 75-144 (New York, NY. Oxford University Press, 2002).
15. Rota M, Padin-Iruegas ME, Misao Y, De Angelis A, Maestroni S, Ferreira-Martins J, Fiumana E, Rastaldo R, Arcarese ML, Mitchell TS, Boni A, Bolli R, Urbanek K, Hosoda T, Anversa P, Leri A, Kajstura J. Local activation or implantation of cardiac progenitor cells rescues scarred infarcted myocardium improving cardiac function. *Circ Res*. 2008; 103: 107-16.
16. Denny WA, Wilson WR. Tirapazamine: a bioreductive anticancer drug that exploits tumour hypoxia. Expert Opin. Investig. Drugs. 2000; 9: 2889-2901.
17. Wilson WR, Hay MP. Targeting hypoxia in cancer therapy. Nat. Rev. Cancer. 2011; 11: 393-410.
18. Rota M, Hosoda T, De Angelis A, Arcarese ML, Esposito G, Rizzi R, Tillmanns J, Tugal D, Musso E, Rimoldi O, Bearzi C, Urbanek K, Anversa P, Leri A, Kajstura J. The young mouse heart is composed of myocytes heterogeneous in age and function. *Circ Res*. 2007; 101: 387-99.
19. Bolli R, Chugh AR, D'Amario D, Loughran JH, Stoddard MF, Ikram S, Beache GM, Wagner SG, Leri A, Hosoda T, Sanada F, Elmore JB, Goichberg P, Cappetta D, Solankhi NK, Fahsah I, Rokosh DG, Slaughter MS, Kajstura J, Anversa P. Cardiac stem cells in patients with ischaemic cardiomyopathy (SCIPIO): initial results of a randomised phase 1 trial. *Lancet*. 2011; 378: 1847-57.
20. Hosoda T, D'Amario D, Cabral-Da-Silva MC, Zheng H, Padin-Iruegas ME, Ogorek B, Ferreira-Martins J, Yasuzawa-Amano S, Amano K, Ide-Iwata N, Cheng W, Rota M, Urbanek K, Kajstura J, Anversa P, Leri A. Clonality of mouse and human cardiomyogenesis in vivo. *Proc Natl Acad Sci U S A*. 2009; 106: 17169 74.
21. Clark JM, Lambertsen CJ. Pulmonary oxygen toxicity: a review. *Pharmacol. Rev*. 1971; 23: 37-133.
22. Jin Y, Kim HP, Chi M, Ifedigbo E, Ryter SW, Choi AM. Deletion of caveolin-1 protects against oxidative lung injury via up-regulation of heme oxygenase-1. *Am. J. Respir. Cell Mol. Biol*. 2008; 39: 171-179.
23. Tanaka A, Jin Y, Lee SJ, Zhang M, Kim HP, Stolz DB, Ryter SW, Choi AM. Hyperoxia-induced LC3B interacts with the Fas apoptotic pathway in epithelial cell death. *Am. J. Respir. Cell Mol. Biol*. 2012;46: 507-514.
24. Orlic D, Kajstura J, Chimenti S, Limana F, Jakoniuk I, Quaini F, Nadal-Ginard B, Bodine DM, Leri A, Anversa P. Mobilized bone marrow cells repair the infarcted heart, improving function and survival. *Proc Natl Acad Sci U S A*. 2001; 98: 10344-9.
25. Kajstura J, Gurusamy N, Ogórek B, Goichberg P, Clavo-Rondon C, Hosoda T, D'Amario D, Bardelli S, Beltrami AP, Cesselli D, Bussani R, del Monte F, Quaini F, Rota M, Beltrami CA, Buchholz BA, Leri A, Anversa P. Myocyte turnover in the aging human heart. *Circ Res*. 2010; 107:1374-86.

Online Table I. Antibodies

Protein	Antibody	Company	Application	Labeling	Fluorochromes
Stem cell marker					
c-kit	goat polyclonal	R&D	IHC	indirect	F
c-kit	rat monoclonal	BD Pharmingen	FACS	direct	F
c-kit	rat polyclonal	R&D	IHC	indirect	F
Lineage marker					
Lin-cocktail	hamster monoclonal	BioLegend	FACS	direct	PE
GATA4	goat polyclonal	Santa Cruz Bio	FACS	indirect	T
Nkx2.5	goat polyclonal	Santa Cruz Bio	FACS	indirect	T
CD45	mouse monoclonal	BD Pharmingen	FACS	direct	APC
Procollagen	goat polyclonal	Santa Cruz Bio	IHC	indirect	T
Structural proteins of myocardial cells					
α-sarcomeric actin	mouse monoclonal	Sigma	IHC	indirect	F, T, Cy5, QD655
Other stainings					
Pimonidazole	rabbit polyclonal	hip	IHC, FACS	indirect	T, Cy5
Pimonidazole	mouse polyclonal	hip	IHC	indirect	Cy5
HIF-1α	rabbit polyclonal	abcom	IHC	indirect	T
CAIX	rabbit polyclonal	Novus Biologicals	IHC	indirect	T
BrdU	mouse monoclonal	Roche	IHC	indirect	F, T
Ki67	rabbit polyclonal	Vector	IHC	indirect	T
Ki67	rat monoclonal	DAKO	FACS	indirect	T
$p16^{INK4a}$	mouse monoclonal	Santa Cruz Bio	FACS	indirect	T
Telomere PNA FISH	N/A	DAKO	QFISH	N/A	Cy3
Nuclear DNA	DAPI		IHC	N/A	

Direct labeling: primary antibody conjugated with the fluorochrome.
Indirect labeling: species-specific secondary antibody conjugated with the fluorochrome.

F: fluorescein isothiocyanate; PE: phycoerythrin; T: tetramethyl rhodamine isothiocyanate; APC: allophycocyanin; Cy: cyanine; QD655: quantum dots with emission at 655 nm.

Online Table II. Magnitude of Sampling

Parameter	n value	Aggregate sample size	Sample size (mean ± SD)
Mitochondria			
Nitroreductase activity assay	3	105[(1)]	35±5
Mito Tracker Green FM	3	234[(1)]	78±16
TMRE	3	230[(1)]	77±14
Pimo-labeled human CSCs			
21%	3	690[(2)]	230±11
10%	3	921[(2)]	307±59.3
5%	3	856[(2)]	285±83
1%	3	659[(2)]	220±21
Pimo staining (IHC)			
Atria			
3 month old	5	62[(3)]	12±5
24 month old	5	109[(3)]	22±4
30 month old	5	108[(3)]	22±2
Base-MR			
3 month old	5	59[(3)]	12±5
24 month old	5	91[(3)]	18±4
30 month old	5	108[(3)]	22±2
Apex			
3 month old	5	63[(3)]	13±5
24 month old	5	122[(3)]	24±3
30 month old	5	133[(3)]	27±9
O_2 diffusion distance			
Young (3 month old)	12	62[(4)]	5±3
Old (30 month old)	23	133[(4)]	6±4
TPZ study			
Young (3 month old)			
Baseline			
Ki67	5	3116[(5)]	623±110
GATA4	4	2465[(5)]	616±112
Nkx2.5	4	2399[(5)]	600±153
CD45	3	1706[(5)]	569±142
Day 1			
Ki67	4	800[(5)]	200±20
GATA4	4	1346[(5)]	337±54
Nkx2.5	6	1820[(5)]	364±68

Day 5			
Ki67	5	1619[(5)]	324±136
GATA4	4	931[(5)]	233±12
Nkx2.5	5	1125[(5)]	225±23
Day 12			
Ki67	4	1700[(5)]	425±42
GATA4	4	1603[(5)]	401±83
Nkx2.5	4	2122[(5)]	424±56
Old (30 month old)			
Baseline			
Ki67	5	2047[(5)]	409±89
GATA4	6	2310[(5)]	385±42
Nkx2.5	5	2122[(5)]	424±56
Day 1			
Ki67	3	630[(5)]	210±87
GATA4	3	563[(5)]	188±13
Nkx2.5	3	728[(5)]	243±22
Day 5			
Ki67	5	1343[(5)]	269±41
GATA4	5	1365[(5)]	273±41
Nkx2.5	4	1324[(5)]	331±184
Day 12			
Ki67	6	1916[(5)]	319±92
GATA4	6	1925[(5)]	321±120
Nkx2.5	6	1705[(5)]	272±72
Thymus			
PBS-treated			
3 month old	7	N/A	N/A
24 month old	6	N/A	N/A
30 month old	6	N/A	N/A
TPZ-treated			
3 month old	7	N/A	N/A
24 month old	8	N/A	N/A
30 month old	6	N/A	N/A
Hemodynamics			
PBS-treated			
3 month old	7	N/A	N/A
30 month old	8	N/A	N/A
TPZ-treated			
3 month old	5	N/A	N/A
30 month old	7	N/A	N/A
Telomere length			
3 month old			

Pimo-pos CSCs	5	371[6]	74±7
Pimo-neg CSCs	5	361[6]	72±13
Myocyte	5	362[6]	72±5
30 month old			
Pimo-pos CSCs	5	368[6]	74±6
Pimo-neg CSCs	5	306[6]	61±16
Myocyte	5	351[6]	70±6
$p16^{INK4a}$			
Young (3 month old)	4	2146[5]	537±102
Old (30 month old)	4	2823[5]	706±142
BrdU pulse chase			
7 days pulse			
Atria	5	66[7]	13.2±4.3
Base-MR	5	81[7]	16.2±5.0
Apex	5	79[7]	15.8±3.3
2 months chase			
Atria	5	72[7]	14.4±5.3
Base-MR	5	75[7]	15.0±3.1
Apex	5	78[7]	15.6±3.2
5 months chase			
Atria	4	50[7]	12.5±3.7
Base-MR	4	53[7]	13.3±4.8
Apex	4	55[7]	13.8±1.9
70% hyperoxia (26 month old)			
CTRL	3	1772[5]	591±53
1 day	3	1421[5]	474±117
7 days	3	1509[5]	503±82
SCF injection			
Pimo labeling (26 month old)			
CTRL	3	1965[5]	655±176
SCF 6hr	3	1775[5]	592±175
SCF 24hr	3	1423[5]	474±99
BrdU labeling of CSCs 2 days			
PBS-treated	4	126[8]	32±2
SCF-treated	4	83[8]	46±3
BrdU labeling of CSCs 21 days			
PBS-treated	5	145[8]	29±3
SCF-treated	5	210[8]	42±6
CSC number 2 days			

PBS-treated	4	126[(1)]	32±2
SCF-treated	4	183[(1)]	46±3
CSC number 21 days			
PBS-treated	5	145[(1)]	29±3
SCF-treated	5	210[(1)]	42±6
BrdU labeling of newly formed myocytes			
PBS-treated	6	638[(9)]	106±7
SCF-treated	7	753[(9)]	108±12
Telomere length of newly formed myocyte s			
PBS-treated	8	273[(9)]	34±13
SCF-treated	8	305[(9)]	38±15
Myocyte nucleation			
PBS-treated	6	960[(10)]	160±45
SCF-treated	7	499[(10)]	71±35
Myocyte volume			
PBS-treated	5	298[(10)]	60±1
SCF-treated	5	288[(10)]	58±5
Cardiac anatomy			
PBS-treated	6	N/A	N/A
SCF-treated	7	N/A	N/A
Hemodynamics			
PBS-treated	5	N/A	N/A
SCF-treated	7	N/A	N/A
Echocardiography			
PBS-treated	5	N/A	N/A
SCF-treated	7	N/A	N/A
Wall stress			
PBS-treated	5	N/A	N/A
SCF-treated	7	N/A	N/A
Circulating hematopoietic cells			
CTRL	3	5155[(11)]	1718±557
PBS-treated	3	8648[(11)]	2883±671
SCF-treated	3	6231[(11)]	2077±959

(1) Total number of mouse CSCs counted.
(2) Total number of human CSCs counted.
(3) Number of CSCs counted for Pimo-positive and -negative.
(4) Aggregate number of capillaries within the radius of 30 mm from CSCs.
(5) Number of CSCs measured by FACS.
(6) Number of cells measured by confocal microscopy.
(7) Number of CSCs counted following BrdU-pulse.

(8) Number of dividing CSCs analyzed by confocal microscopy.
(9) Number of newly-formed myocytes.
(10) Total number of myocyte analyzed by confocal microscopy for the measurement of myocyte nucleation or volume.
(11) Number of circulating ckit-positive hematopoietic cells measured by FACS.

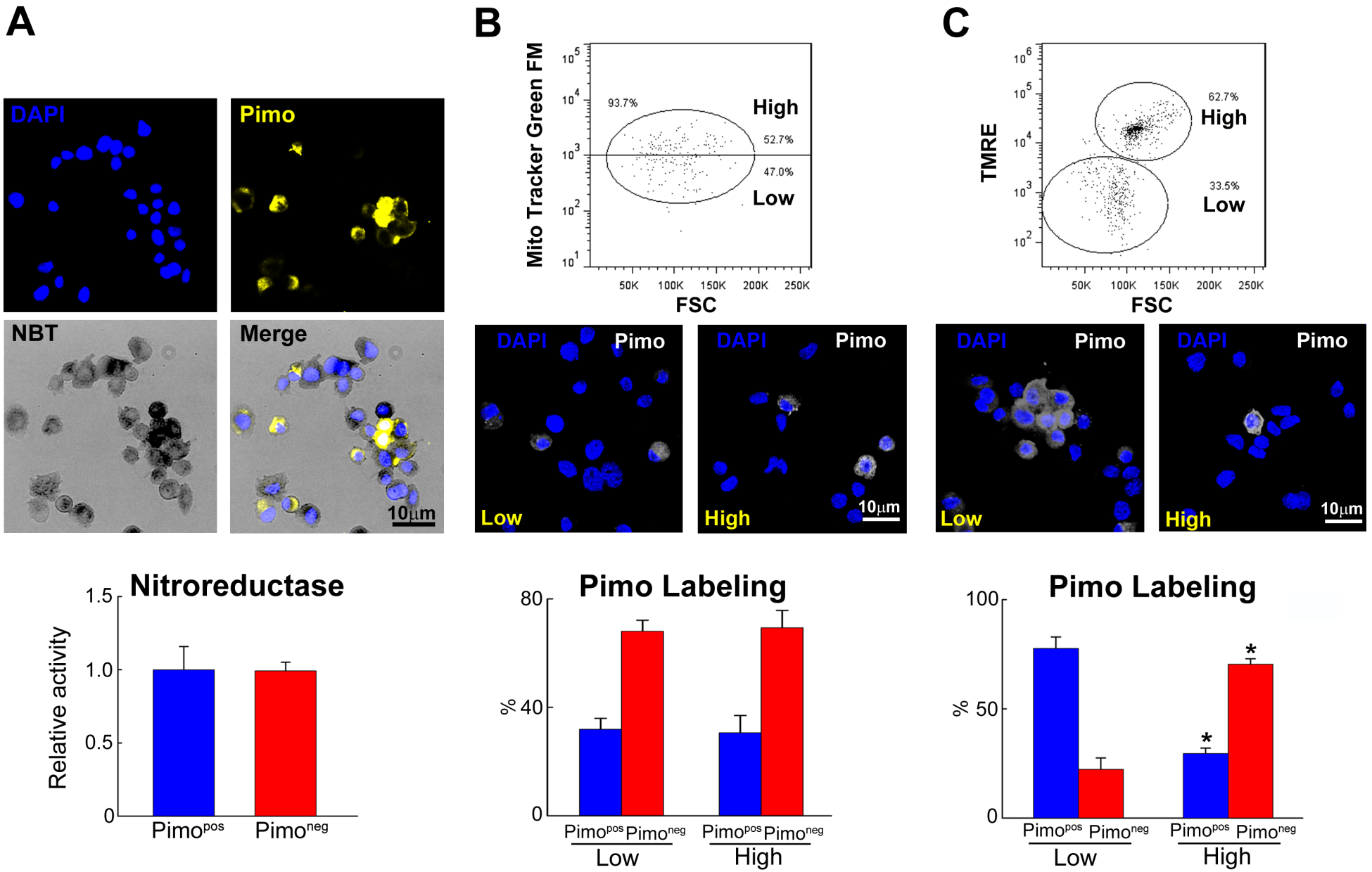

Online Figure I. A-C

A

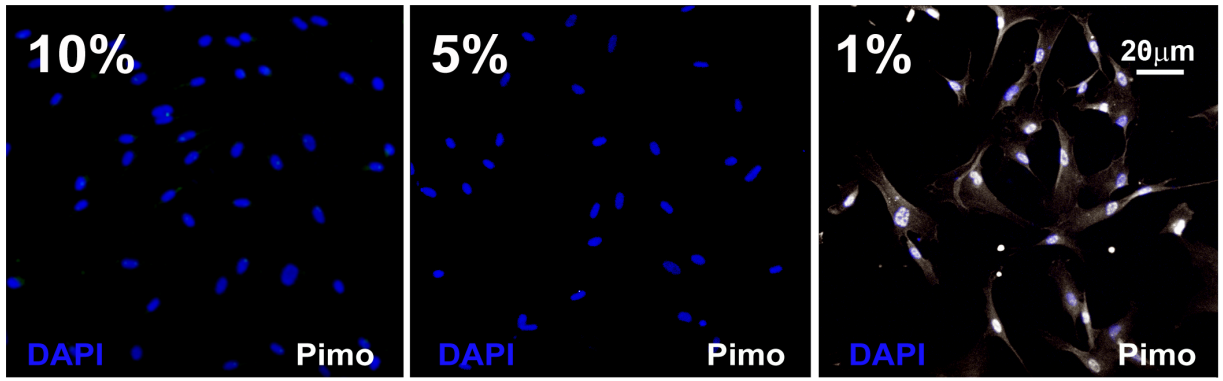

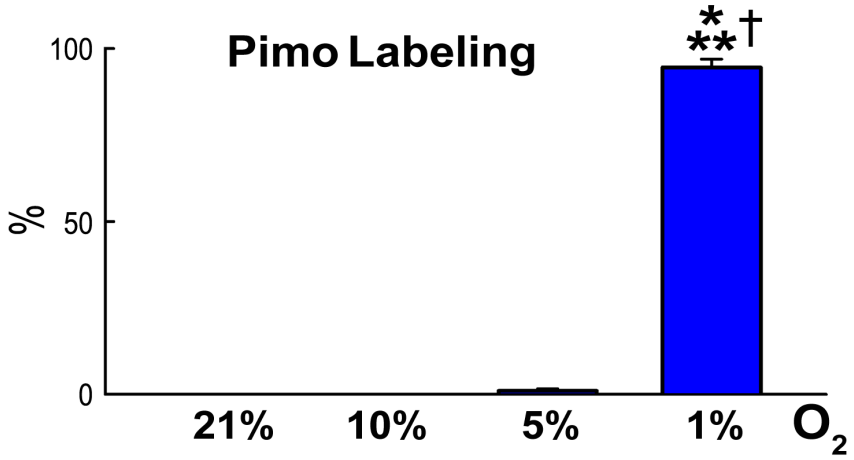

Online Figure II. A

B

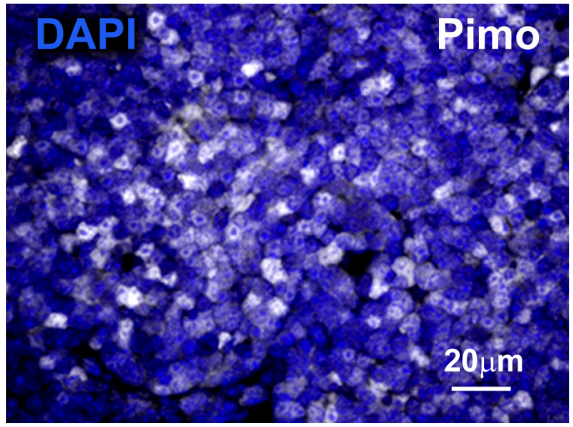

C

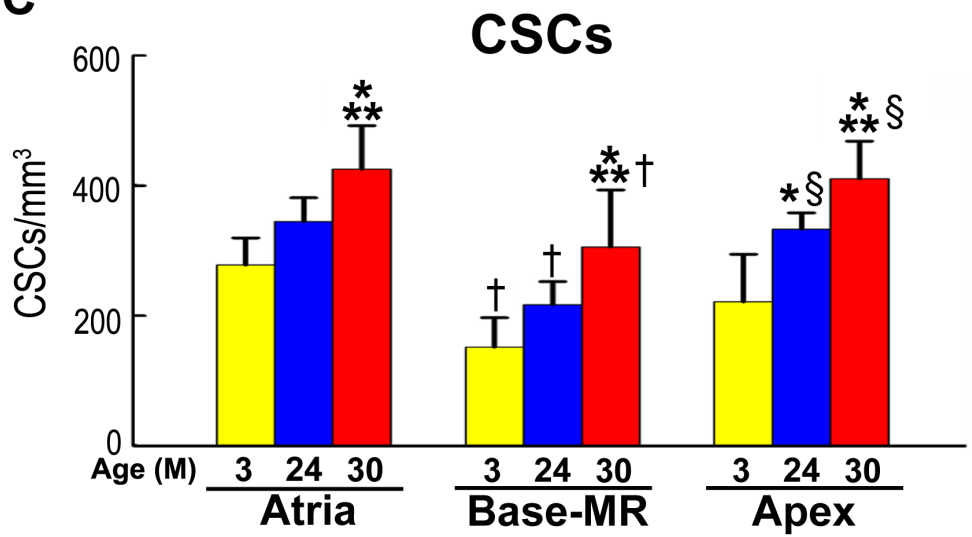

Online Figure II. B, C

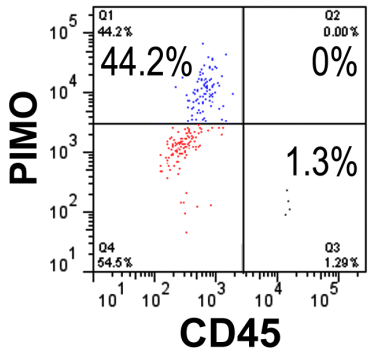

Online Figure III.

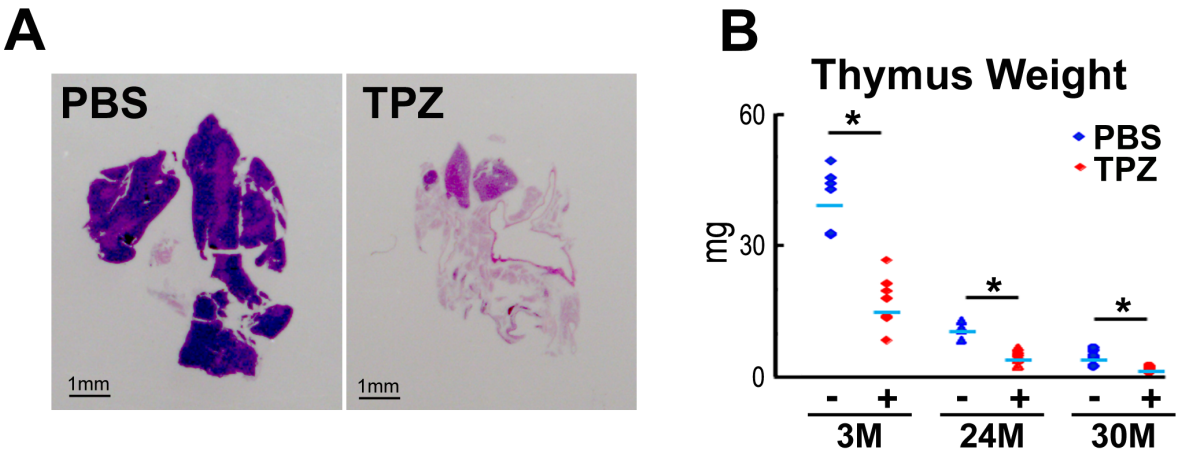

Online Figure IV.

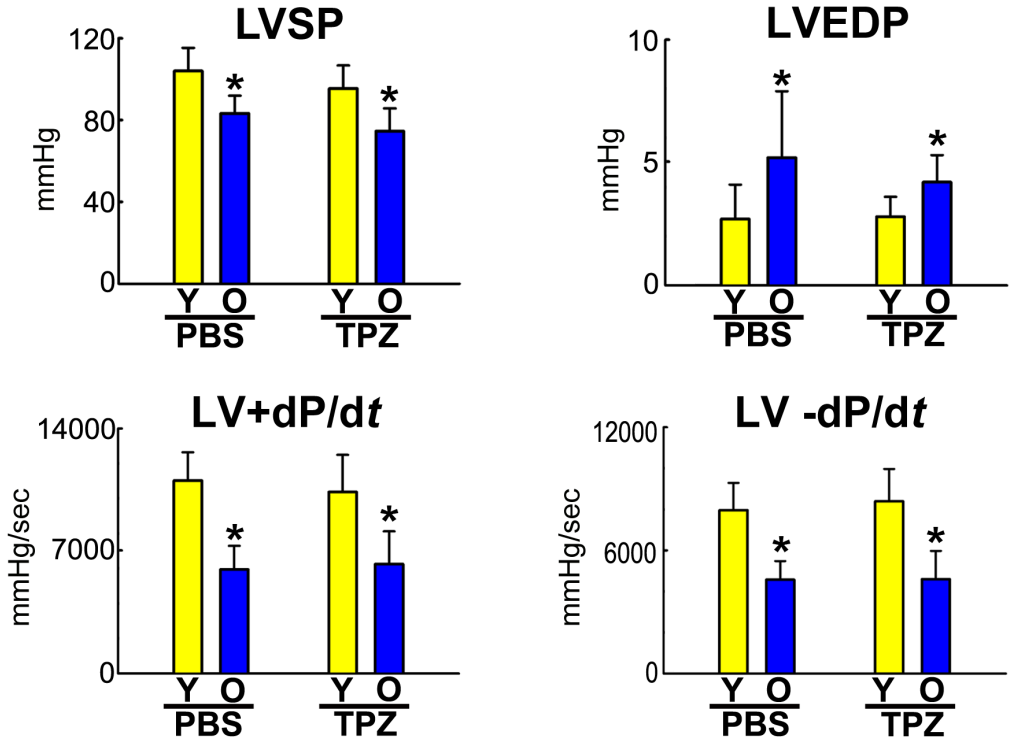

Online Figure V.

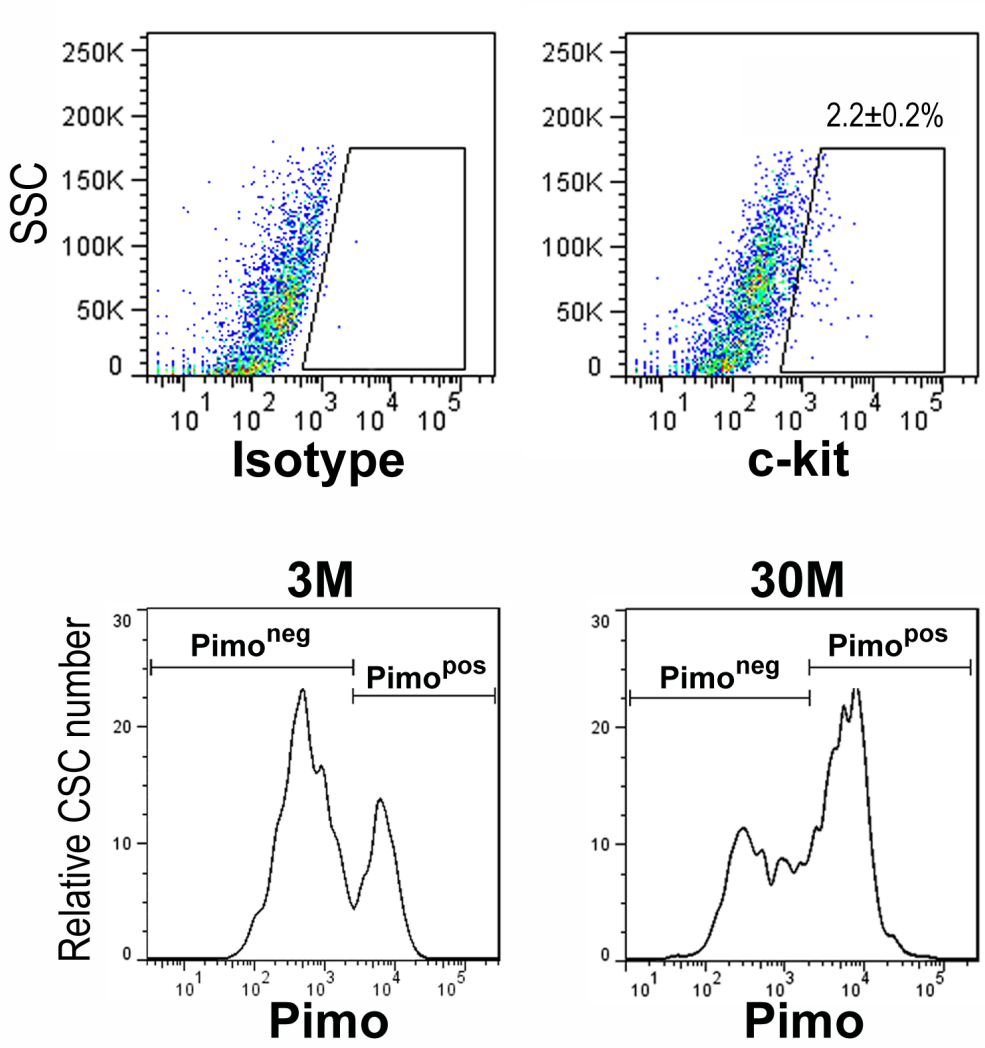

Online Figure VI.

Negative control

area (μm^2)	mean intensity	area x mean intensity
41.5	17.8	739.0
42.1	14.4	604.7
49.0	17.5	857.8
44.6	16.5	736.9
41.0	21.5	879.0
42.2	20.6	870.3
35.1	23.4	820.8
34.1	22.6	771.6
43.0	21.3	913.8
28.6	22.2	633.4
28.2	22.8	643.8
28.6	20.5	587.7

Online Figure VII.

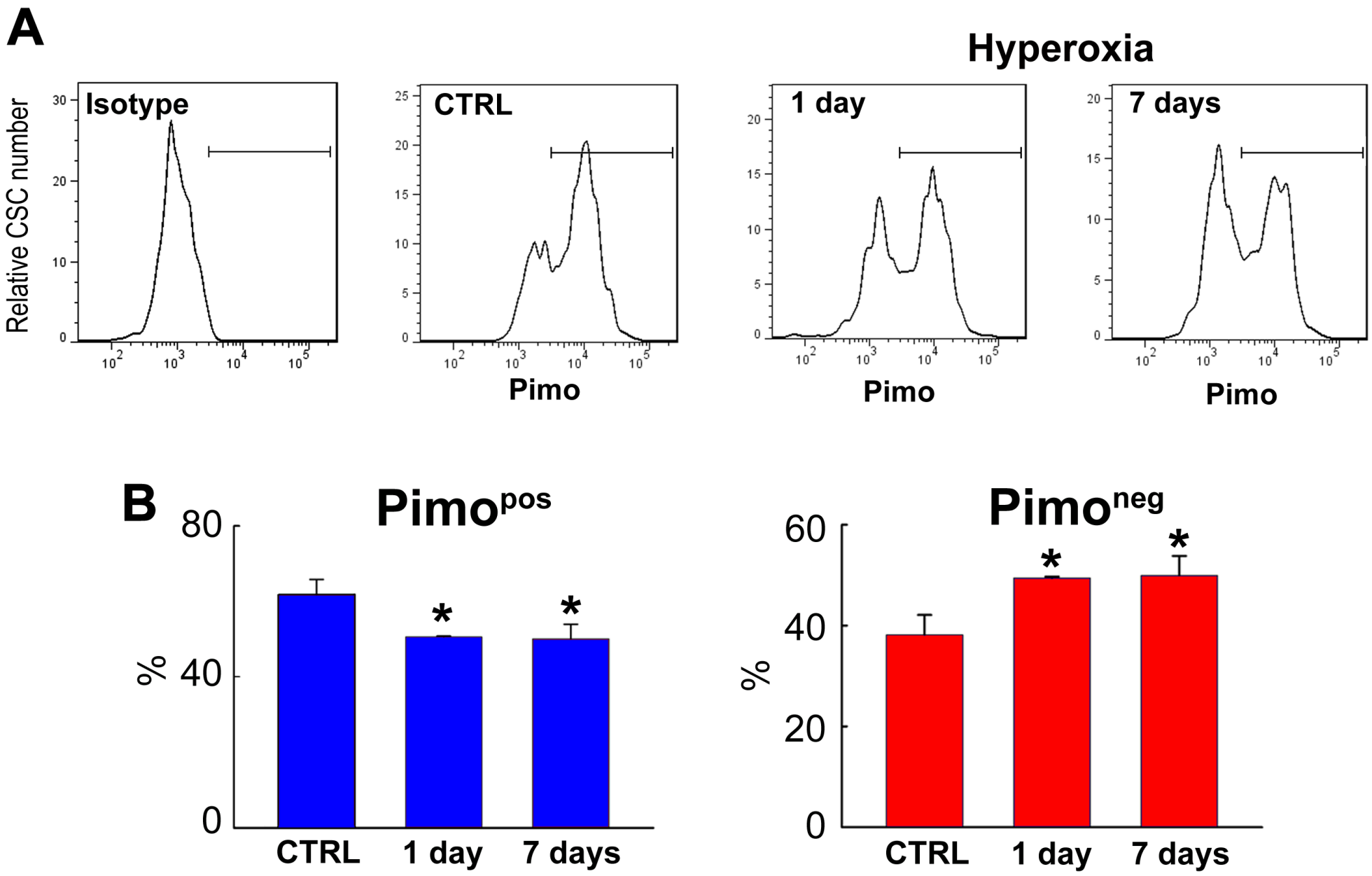

Online Figure. VIII. A, B

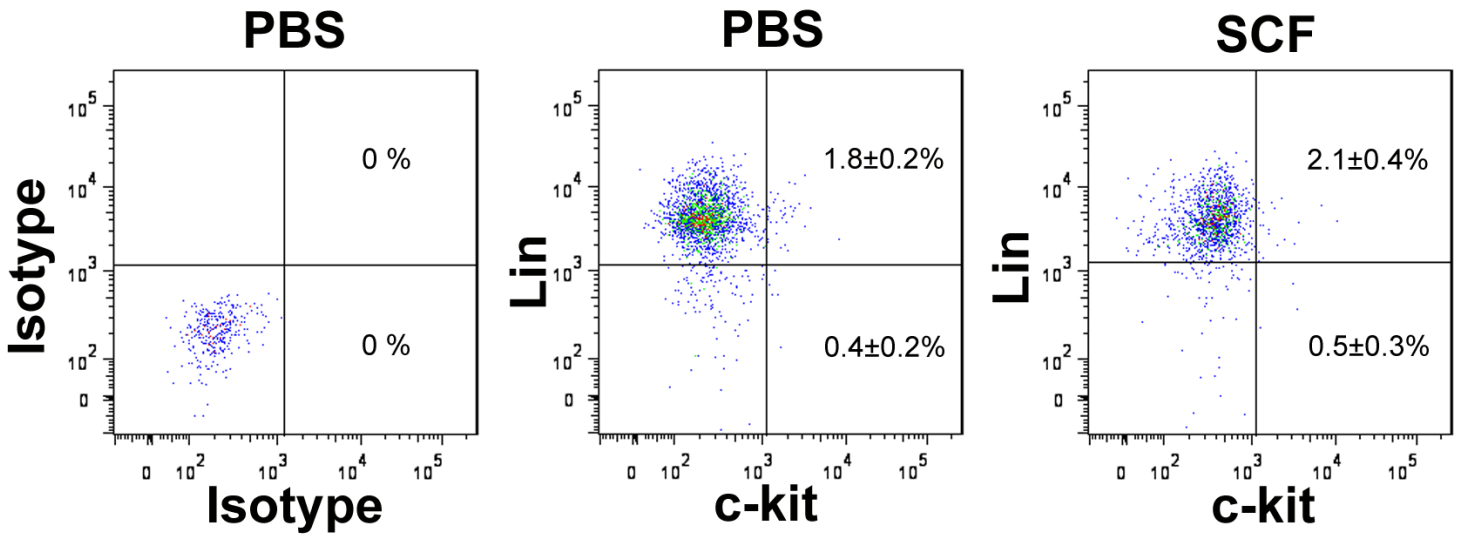

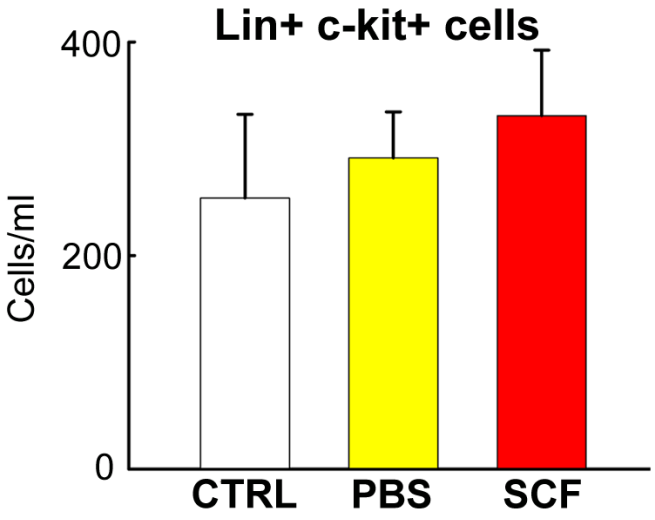

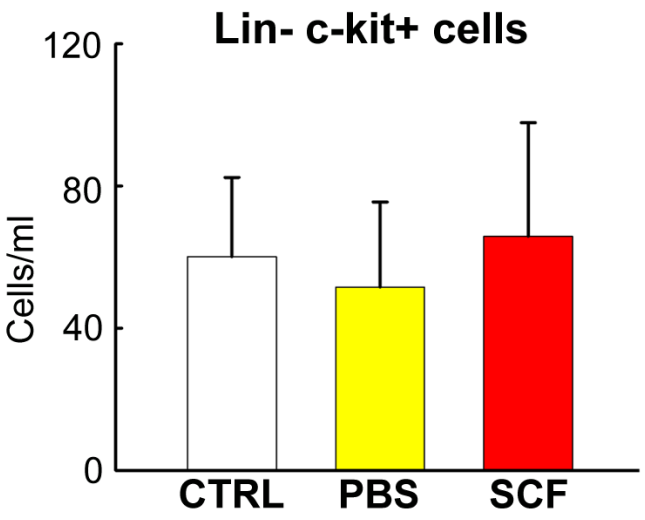

Online Figure IX.

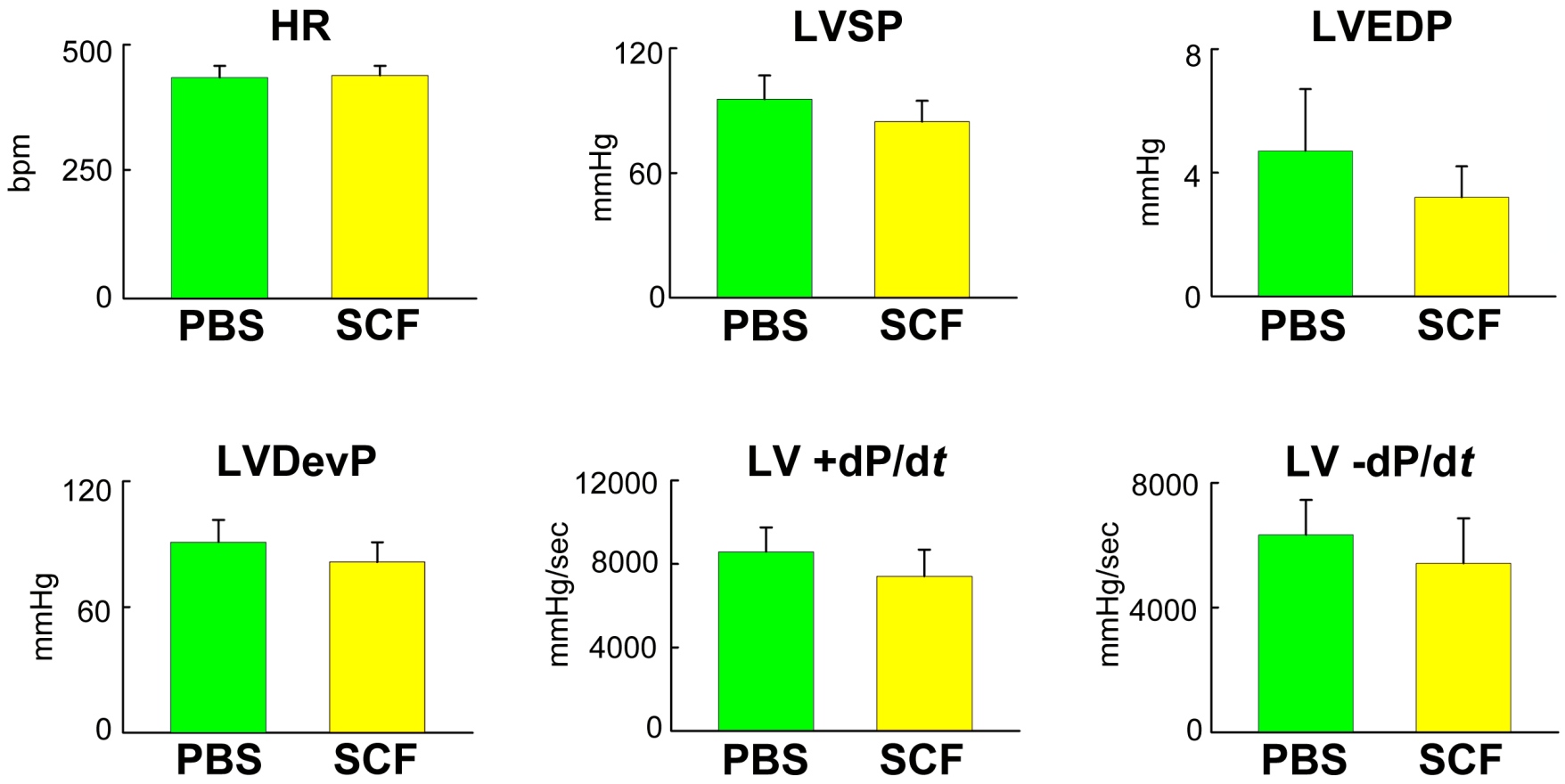

Online Figure X.

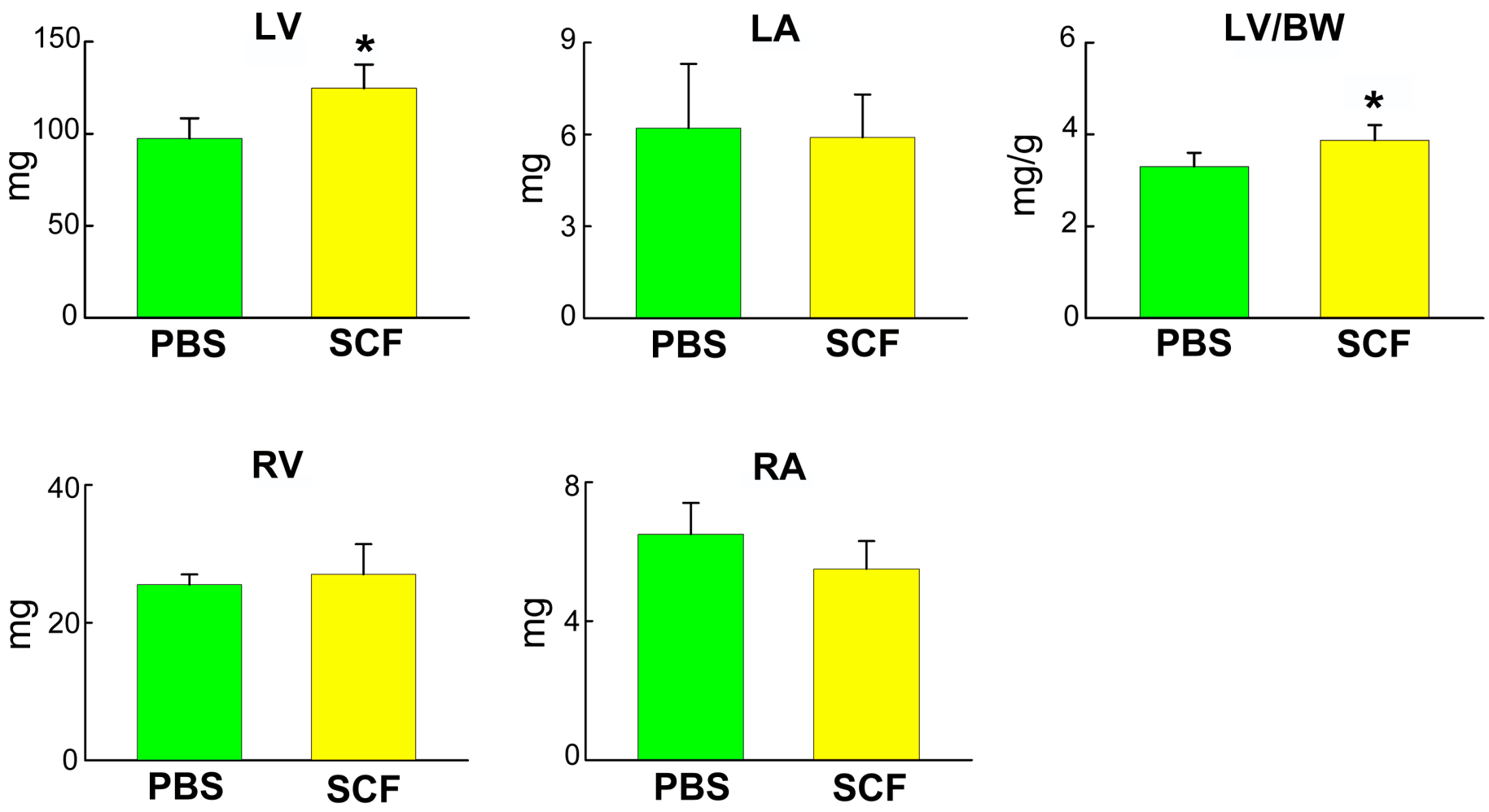

Online Figure XI.

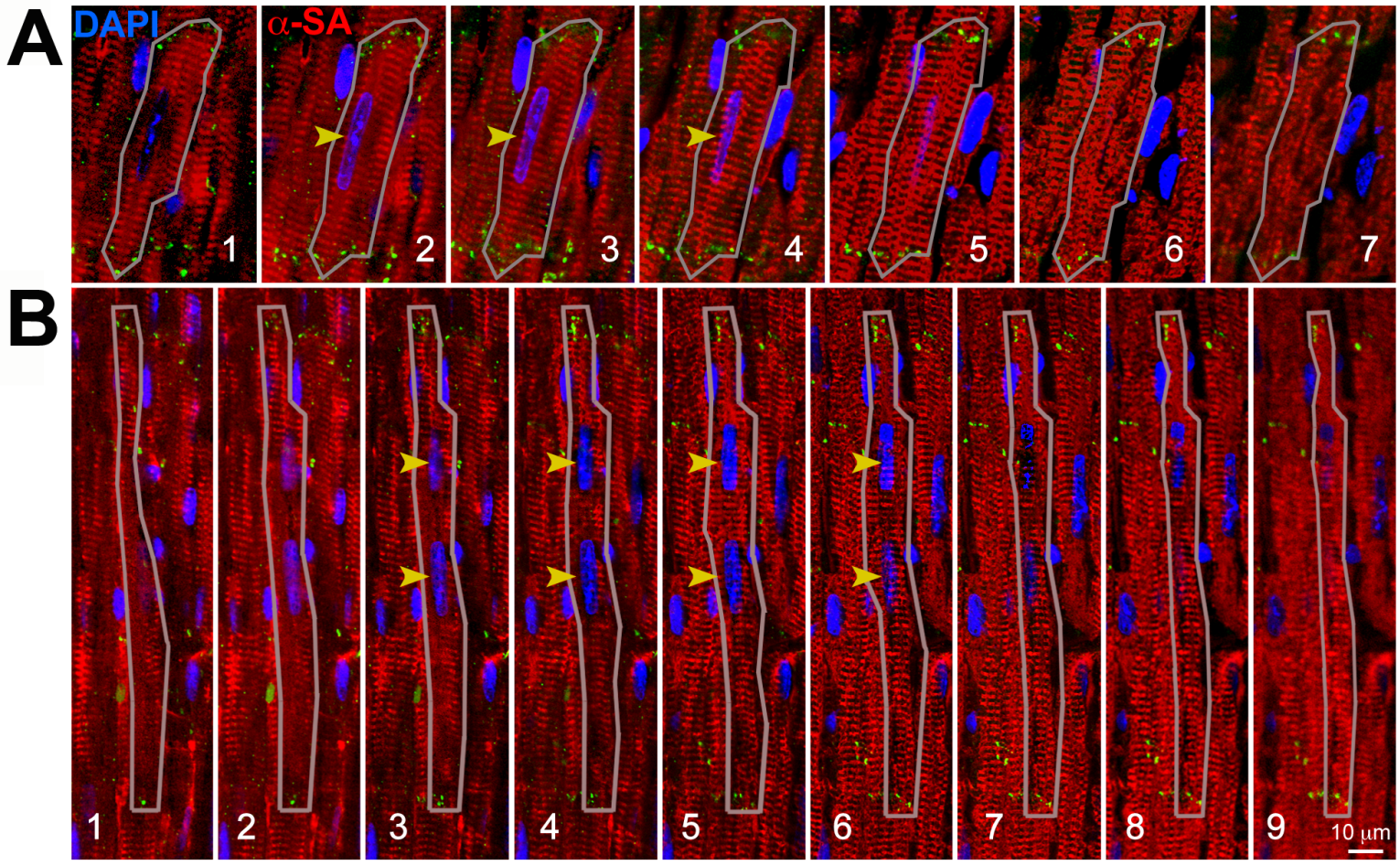

Online Figure XII. A, B